Chem Biol Drug Des 2012; **79:** 628–638

Research Article

doi: 10.1111/j.1747-0285.2012.01342.x

Synthesis, Molecular Docking, and Biofilm Formation Inhibitory Activity of 5-Substituted 3,4-Dihalo-5*H*-furan-2-one Derivatives on *Pseudomonas aeruginosa*

Guo-Yong Liu†, Bao-Qin Guo†, Wan-Na Chen, Chao Cheng, Qian-Lan Zhang, Mi-Bei Dai, Jun-Rong Sun, Ping-Hua Sun and Wei-Min Chen*

Guangdong Province Key Laboratory of Pharmacodynamic Constituents of TCM and New Drugs Research, College of Pharmacy, Jinan University, Guangzhou 510632, China
**Corresponding author: Wei-Min Chen, twmchen@jnu.edu.cn*
†These authors contributed equally to this work.

***Pseudomonas aeruginosa* (*P. aeruginosa*) colonize on most wounds and live as biofilm, which causes antibiotic resistance and wounds unhealed. To investigate the effects of 5-substituted 3,4-dihalo-5*H*-furan-2-one compounds on biofilm formation of *P. aeruginosa,* a set of 5-(aryl-1′-hydroxy-methyl)- or 5-(aryl-2-methylene)-3,4-dihalo-5*H*-furan-2-one compounds were designed and synthesized. Their inhibitory activities on biofilm formation of *P. aeruginosa* were studied by MIC assay, quantitative analysis of biofilm inhibition, and observation of biofilm formation with SEM. It was found that compounds 2i, 3f, 3i showed remarkable effects of biofilm formation inhibition on *P. aeruginosa*. Furthermore, molecular docking was performed to identify the key structural features of these compounds with the binding site of LasR receptor.**

Key words: biofilm, docking, furanone, *Pseudomonas aeruginosa*, quorum sensing

Received 14 January 2011, revised 8 December 2011 and accepted for publication 24 December 2011

The bacterium produce, release, and detect the autoinducers (AI) to engage in multicellular behavior and co-ordinate gene expression with some changes of physiology such as biofilm formation and virulence factor secretion. This chemical communication among bacterium is called quorum sensing (QS) (1). *Pseudomonas aeruginosa* are found in most chronic wounds (2,3). They colonized in this specialized surface, living as a biofilm style (4,5) with the help of quorum-sensing communication, and they may cause serious antibiotics resistance and immunology dysfunction of bodies (2,6,7). As wounds are easily colonized by bacterium, infection has been regarded as one of the most important factors that aggravate wounds and even make them unhealed (8).

Developing the QS antagonists, which can block the QS system of *P. aeruginosa* with the mechanism of reducing biofilm formation and virulence factor secretion, is a new strategy to counteract bacterial infection. The *N*-acyl homoserine lactones (AHLs) were identified as the QS autoinducer-1 (AI-1) of *P. aeruginosa* by the way of binding with key receptor LasR to form complex-complex dimeride and then combine on the definite site of DNA that eventually resulted in changes of gene transcription (9). The natural furanones (**a, b**) isolated from the macro-algae *Delisea pulchra* are revealed to be inhibitors of biofilm formation for several bacterial species, and their analogues (**c, d**) have also been found to be potential inhibitors (10–13).

Recent study (14) has revealed that vinyl bromide moiety of brominated furanones is essential for their quorum-sensing-inhibitory activities. The ring vinyl bromide was proposed to covalently modify and inactivate LuxS. The LuxS is a key enzyme in biomass producing autoinducer-2 (AI-2) that was the signal of both Gram-negative and Gram-positive bacterium QS systems. Once the path of AI-2 agonist was interfered, the QS system may be blocked to a large extent. It was reported (15) that AHLs modified with substituted aromatic nucleus would exhibit a remarkable improvement for quorum-sensing-inhibitory effect.

Based on scientific evidences as mentioned earlier, we aim to develop a series of new QS inhibitors targeted to both LasR and LuxS receptors simultaneously. To increase the potency of inhibition of bacterial biofilm formation, 3, 4-dihalo-2(5*H*)-furanones were modified by introducing substituted aromatic groups. The 5-(aryl-1′-hydroxy-methyl)- or 5-(aryl-2-methylene)-3,4-dihalo-5*H*-furan-2-one compounds were synthesized (Schemes 1 and 2). In this paper, all the synthesized compounds were evaluated by biological test of biofilm formation inhibitory activities against *P. aeruginosa*. Moreover, to explore and identify the binding mode between these inhibitors and the LasR receptor, a systemic molecular docking experiment was also carried out.

Materials and Methods

Chemistry

All reagents and solvents were purchased from commercial sources. Further purification and drying by standard methods were employed if necessary. CH_3OH and THF were distilled from CaH_2, and Et_3N

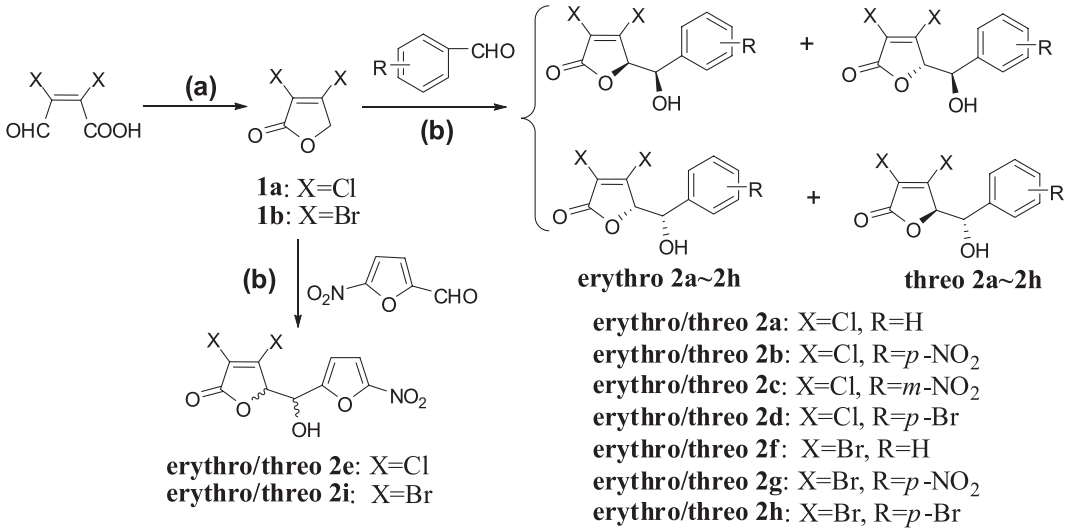

Scheme 1: Synthesis of 5-(aryl-1′-hydroxy-methyl)-3,4-dihalo-5*H*-furan-2-ones. Conditions: (a) CH_3OH, $NaBH_4$, −2 °C, 15 min, then con. H_2SO_4, −2 °C, 30 min; (b) Et_3N, CH_3OH, r.t., 4 h.

was distilled from sodium. The thin-layer chromatographic analyses were performed on silica gel plates (Qingdao haiyang GF_{254}, Qingdao, China) and visualized under UV light. All NMR spectra were recorded on Mercury-300, Mercury-400, or Mercury-500 spectrometers in d_6-DMSO, $CDCl_3$, or CD_3OD. Electrospray ionization mass spectra (ESI-MS) were obtained on a Finnigan LCQ Advantage MAX mass spectrometer [Applied Biosystems, (Carlsbad, CA, USA) 4000 Q TRAP]. High-resolution mass spectra were obtained on an Aglient 6210 series LC/MSD TOF mass spectrometer.

Two chiral carbons in compounds **2a–2h** resulted in formed four compounds with two kinds of configurations. The one with big groups on the same side is erythro isomer, while the one on different side is threo isomer.

As ^{1}H-NMR signal strength of compound is in accordance with the amount of hydrogen positively, the ratio of erythro and threo compounds could be determined by ^{1}H-NMR. It was reported (16) that the ^{1}H-NMR chemical shift of erythro compounds was obviously larger than the threo ones such as compound **4ba** (Figure 1). In this study, both erythro and threo compounds were confirmed by ^{1}H-NMR spectra comparison with literatures, and the ratio of erythro to threo were also determined by the integral ratios. For example, ^{1}H-NMR chemical shifts of erythro-**2c** and threo-**2c** were classified as Figure 2A,B. Their ratio was calculated as follows: ratio (erythro-**2c**:/threo-**2c**) = 1.00/(1.00 + 0.46): 0.46/(1.00 + 0.46) = 68:32. As erythro and threo conformation were diastereomer, the ratio was also named as diastereomeric ratio (dr) (17).

The configuration of (*Z*)/(*E*)-**3a**–**3i** isomers were confirmed according to the literature (18). The ratios of erythreo/threo or (*Z*)/(*E*) isomers were assigned by analyzing ^{1}H NMR spectra of compounds as reported (19,20).

General synthetic procedures of compounds

The (*Z*)-2,3-dihalo-4-oxobut-2-enoic acids were treated with $NaBH_4$ and con.H_2SO_4 to give the key intermediates **1a,b**, according to the literature (21). As shown in Scheme 1, compounds **2a–i** were obtained by an aldol reaction of compound **1a** or compound **1b** with aldehydes, according to literatures (17,22). The synthetic routes of the target compounds **3a**–**i** were shown in Scheme 2. The diastereoisomer ratios of synthetic products were shown in Table 1, and cis/trans isomer ratios of products were shown in Table 2.

3,4-Dichloro-2(5*H*)-furanone (1a)

Yield 95%. ^{1}H NMR (500 MHz, $CDCl_3$): δ 4.90 (s, 2H). ^{13}C NMR (125 MHz, $CDCl_3$): δ 167.4, 150.7, 122.5, 78.6. MS (ESI) *m/z* 153 $(M + H)^+$.

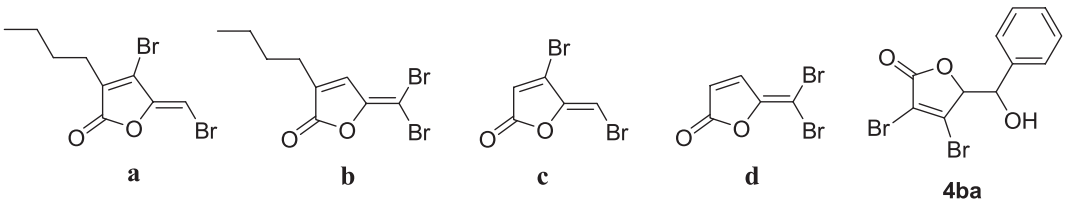

Figure 1: Natural and synthesized halogenated furanones.

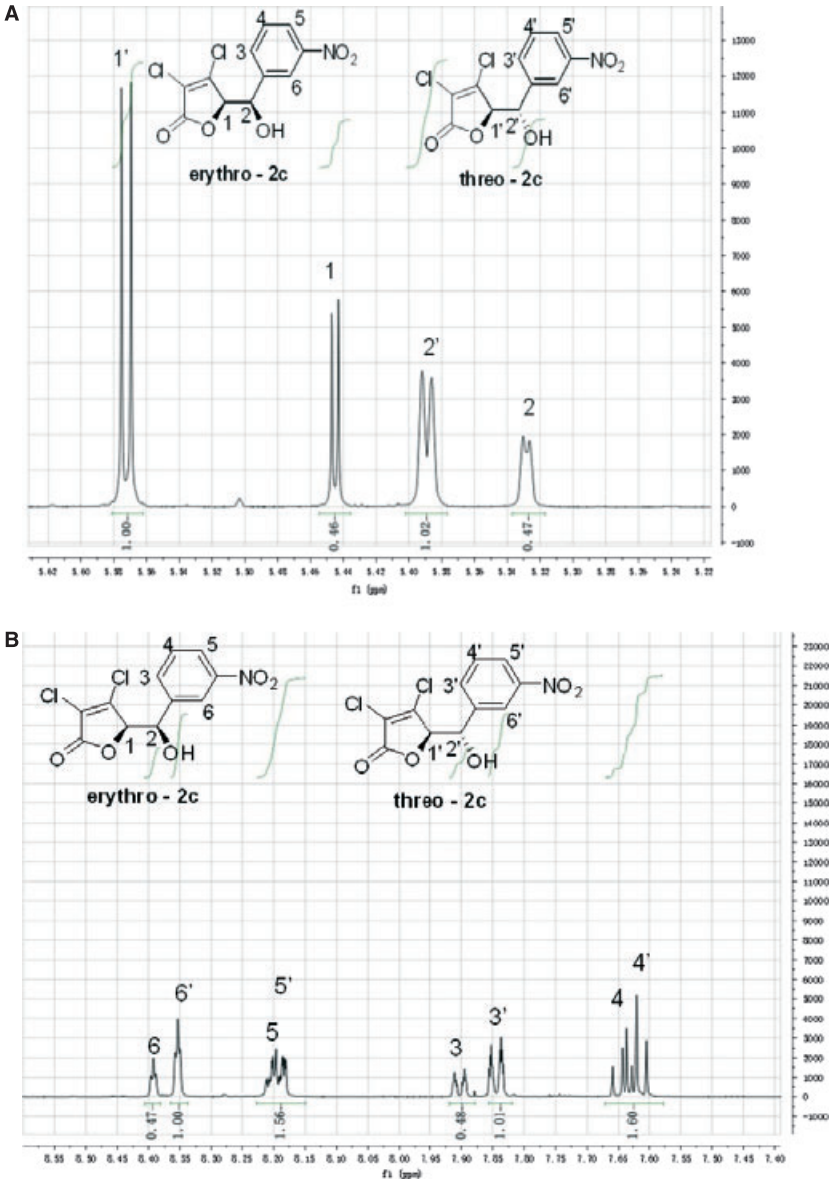

Figure 2: (A) Ratio of erythro and threo **2c** isomers analyzed by ^{1}H-NMR. (B) Ratio of erythro and threo **2c** isomers analyzed by ^{1}H-NMR.

3, 4-Dibromo-2(5*H*)-furanone (1b)

Yield 90%. ^{1}H NMR (300 MHz, $CDCl_3$) δ: 4.86 (s, 2H). MS (ESI) *m/z* 241 $(M + H)^+$.

3,4-Dichloro-5-(hydroxyl(phenyl) methyl)furan-2(5*H*)-one (2a, dr = 96:4)

Yield 90%. ^{1}H NMR (300 MHz, CD_3OD) δ: 7.15–7.30 (m, 5H), 5.48 (d, J = 2.5 Hz, 0.96H), 5.33(d, J = 2.5 Hz, 0.04H), 5.24 (d, J = 2.0 Hz, 0.96H), 5.16 (d, J = 2.0 Hz, 0.04H), 5.05(s, 0.04H), 4.88(s, 0.96H). ^{13}C NMR (75 MHz, CD_3OD) δ : 151.4, 138.0, 130.8, 129.5, 129.3, 128.0, 122.9, 86.9, 73.8. MS (ESI) *m/z* 258 $[M-H]^-$.

3,4-Dichlro-5-(hydroxy(4-nitrophenyl)methyl) furan-2(5*H*)-one (2b, dr = 59:41)

Yield 40%. ^{1}H NMR (500 MHz, CD_3OD) δ: 8.10–8.30 (m, 2H), 7.60–7.85 (m, 2H), 5.57 (d, J = 3.0 Hz, 0.41H), 5.43 (d, J = 2.0 Hz, 0.59H), 5.38 (d, J = 3.0 Hz, 0.41H), 5.31 (d, J = 1.5 Hz, 0.59H). ^{13}C NMR (125 MHz, CD_3OD) δ : 167.1, 152.0, 149.2, 148.7, 129.1, 123.3, 86.6, 70.8. MS (ESI) *m/z* 303 $[M-H]^-$.

3,4-Dichlro-5-(hydroxy(3-nitrophenyl)methyl)furan-2(5*H*)-one (2c, dr = 68:32)

Yield 50%. ^{1}H NMR (500 MHz, CD_3OD) δ: ^{1}H NMR (500 MHz, $CDCl_3$) δ: 8.39 (t, J_1 = 2.0 Hz, J_2 = 0.5 Hz, 0.32H), 8.36 (t, J_1 = 2.0 Hz, J_2 = 0.5 Hz, 0.68H), 8.15–8.23 (m, 1H), 7.9 (m, 0.32H), 7.85 (m, 0.68H), 7.59–7.68 (m, 1H), 5.57 (d, J = 3.0 Hz, 0.68H), 5.45 (d, J = 2.0 Hz, 0.32H), 5.39 (d, J = 3.0 Hz, 0.68H), 5.33 (d, J = 2.0 Hz, 0.32H). ^{13}C NMR (125 MHz, CD_3OD) δ : 167.1, 152.1, 149.8, 141.7, 134.1, 130.8, 124.2, 123.4, 122.8, 86.6, 72.6. MS (ESI) *m/z* 303 $[M-H]^-$.

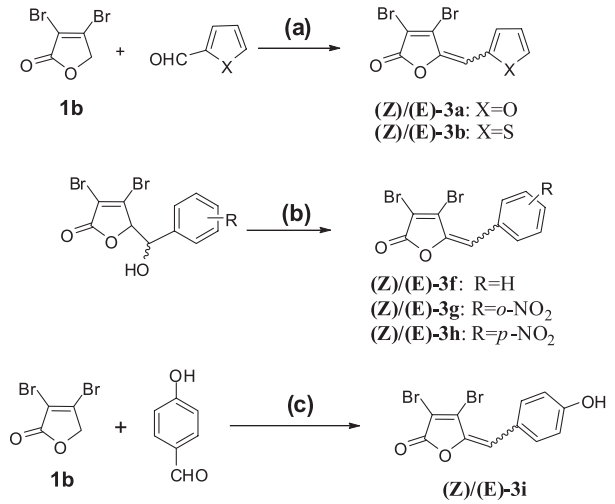

Scheme 2: Synthesis of 5-(aryl-2-methylene)-3,4-dihalo-5*H*-furan-2-ones. Conditions: (a) Et_3N, CH_3OH, r.t., 4 h, then HCl; (b) CH_3OH, H_2SO_4, 86 °C, 8 h; (c) piperidine, toluene, reflux, 1.5 h.

3,4-Dichlro-5-(4-nitrofuran-2-yl(hydroxy)methyl)furan-2(5*H*)-one (2d, dr = 52:48)

Yield 80%. ^{1}H NMR (500 MHz, $CDCl_3$) δ: 7.32–7.38 (m, 1H), 6.81 (dd, J_1 = 4.0 Hz, J_2 = 0.1 Hz, 0.52H), 6.73 (dd, J_1 = 3.5 Hz, J_2 = 0.1 Hz, 0.48H), 5.52 (d, J = 3.0 Hz, 0.52H), 5.43 (m, 0.52H), 5.40 (d, J = 2.0 Hz), 5.29 (m, 0.48H), 3.94 (s, 1H). ^{13}C NMR (125 MHz, $CDCl_3$) δ : 164.5, 153.4, 152.4, 147.7, 121.8, 111.6, 111.1, 81.8, 64.5. MS (ESI) *m/z* 294 $[M-H]^-$.

3,4-Dichlro-5-(hydroxy(4-bromophenyl)methyl)furan-2(5*H*)-one (2e, dr > 99:1)

Yield 42%. ^{1}H NMR (300 MHz, $CDCl_3$) δ: 7.4–7.5 (m, 2H), 7.2–7.3 (m, 2H), 5.28 (d, J = 3 Hz, 1H), 5.23 (d, J = 3 Hz, 1H), 4.89 (s, 1H). MS (ESI) *m/z* 337.3 $[M-H]^-$.

3,4-Dibromo-5-(hydroxyl(phenyl)methyl)furan-2(5*H*)-one (2f, dr = 3:97)

Yield 70%. ^{1}H NMR (400 MHz, $CDCl_3$) δ: 7.34–7.47(5H, m), 5.34(d, J = 2.4 Hz, 0.03H), 5.15(d, J = 2.1 Hz, 0.97H), 5.28(d, J = 2.4 Hz, 0.03H), 5.10(d, J = 2.2 Hz, 0.97H), 3.08(s, 0.03H), 2.16(s, 0.97H); ^{13}C NMR(100 MHz, $CDCl_3$) δ: 165.7, 144.8, 137.6, 128.6, 128.4, 126.3, 115.6, 85.6, 71.6. MS (ESI) *m/z* 349 $[M + H]^+$.

3,4-Dibromo-5-(hydroxy(4-nitrophenyl)methyl)furan-2(5*H*)-one (2g, dr = 23:77)

Yield 38%. ^{1}H NMR (500 MHz, CD_3OD) δ: 8.11–8.17(m, J = 7.5 Hz, J = 2 Hz, 2H), 7.59–7.65(dd, J = 7.5 Hz, J = 2 Hz, 2H), 5.47(d, J = 2.5 Hz, 0.23H), 5.32(d, J = 2.5 Hz, 0.77H), 5.29(d, J = 2.0 Hz, 0.23H), 5.23(d, J = 2.0 Hz, 0.77H); ^{13}C NMR (125 MHz, CD_3OD) δ:

Table 1: Yields and diastereoisomer ratios of the products erythro and threo-**2a**–**2i**

Compound	Product	Yield (%)	Erythro/threo[a]
Erythro/threo-**2a**	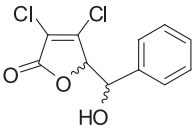	90	96:4[b]
Erythro/threo-**2b**	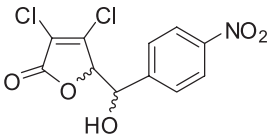	40	59:41[b]
Erythro/threo-**2c**	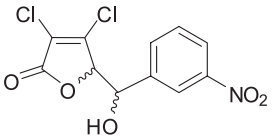	50	68:32[b]
Erythro/threo-**2d**	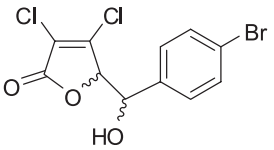	80	52:48[b]
Erythro/threo-**2e**	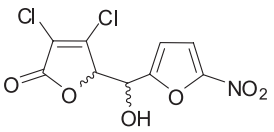	42	>99:1[b]
Erythro/threo-**2f**	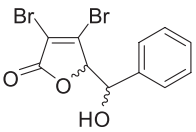	70	3:97[b]
Erythro/threo-**2g**	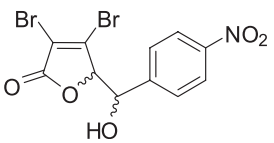	38	23:77[b]
Erythro/threo-**2h**	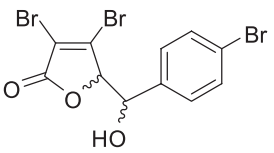	30	5:95[b]
Erythro/threo-**2i**	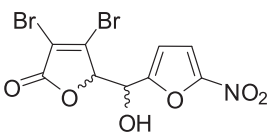	40	36:64[b]

[a]Erythro/threo ratios were determined by NMR.
[b]Erythro/threo isomers were not separated.

Table 2: Yields and cis/trans isomer ratios of (*Z*) and (*E*)-**3a**–**3i**

Compound	Product	Yield (%)	(*Z*)/(*E*)[a]
(*Z*)/(*E*)-**3a**	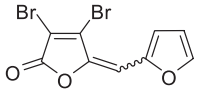	39	99:1[c]
(*Z*)/(*E*)-**3e**	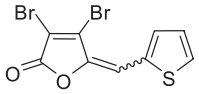	40.5	92:8[c]
(*Z*)/(*E*)-**3f**	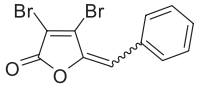	60	10:90[c]
(*Z*)/(*E*)-**3g**	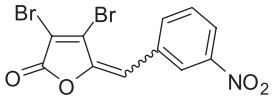	60	57:43[c]
(*Z*)/(*E*)-**3h**	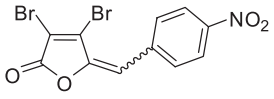	61	82:18[b,c]
(*Z*)/(*E*)-**3i**	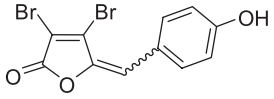	29	ND

[a](*Z*)/(*E*)-ratios were determined by NMR.
[b](*Z*)/(*E*)-ratios were determined by high performance liquid chromatography.
[c](*Z*)/(*E*) isomers were not separated.
ND: (*Z*)/(*E*) isomers were not determined.

168.1, 149.2, 147.6, 146.6, 129.2, 124.3, 116.4, 89.1, 71.1. MS (ESI) *m/z* 393 $[M + H]^+$.

3,4-Dibromo-5-(hydroxy(4-bromophenyl)methyl)furan-2(5*H*)-one (2h, dr = 5:95)

Yield 30%. ^{1}H NMR (500 MHz, d_6-DMSO) δ: 7.55(m, 2H), 7.43(m, 2H), 6.34(s, 0.05H), 6.11(s, 0.95H), 5.63(d, J = 2.0 Hz, 0.05H), 5.51(d, J = 2.0 Hz, 0.95H), 5.16(s, 0.05H), 5.10 (s, 0.95H). ^{13}C NMR (125 MHz, d_6-DMSO) δ: 169.3 150.5, 142.6, 133.7, 131.6, 123.6, 117.0, 90.4, 71.8. MS (ESI) *m/z* 427 $[M + H]^+$.

3,4-Dibromo-5-(4-nitrofuran-2-yl(hydroxy)methyl)furan-2(5*H*)-one (2i, dr = 36:64)

Yield 40%. ^{1}H NMR (400 MHz, $CDCl_3$) δ: 7.50–7.80(m, 0.72H), 7.28–7.36(m, 1.28H), 6.79(d, J = 3.2 Hz, 0.64H), 6.70(d, J = 3.2 Hz, 0.36H), 5.48(d, J = 2.4 Hz, 0.36H), 5.39(d, J = 2.4 Hz, 0.36H), 5.35(d, J = 2.0 Hz, 0.64H), 5.30(s, 0.64H). ^{13}C NMR(100 MHz, $CDCl_3$)δ: 153.7, 143.2, 130.5, 128.4, 116.3, 111.7, 84.1, 67.2, 65.5. MS (ESI) *m/z* 382.3 $[M-H]^-$.

General synthetic procedures of compounds 3a and 3e

To a solution of 3, 4-dibromo-2(5*H*)-furanone (**1b**) (0.24 g, 1.0 mmol) in anhydrous CH_3OH (7 mL) were added Et_3N (0.043 g, 0.1 mmol) and 2-furaldehyde (0.15 g, 1.1 mmol). The mixture was stirred at room temperature for 4 h under nitrogen and then the mixture was concentrated in vacuo. The residue was washed with 5% HCl, exacted with CH_2Cl_2 (20 mL × 3), washed with brine, dried over Na_2SO_4, and concentrated in vacuo. The residue was purified by column chromatography on silica gel using ethyl acetate/petroleum ether (1:15) as the eluent to give compound **3a** (0.12 g, yield 39%) as a yellow solid. The compound **3e** (0.067 g, yield 40.5%) was prepared as a yellow solid using the same method of compound **3a**.

3,4-Dibromo-5-(2-furanylmethylene)-furan-2(5*H*)-one (3a, dr = 1:99)

Yield 39%. ^{1}H NMR (500 MHz, $CDCl_3$) δ: 7.59(d, J = 1.5 Hz), 7.11 (d, J = 3.5 Hz, 1H), 6.58 (dd, 1H, J = 3.5 Hz, 1.5 Hz), 6.47 (s, 1H). ^{13}C NMR (125 MHz, $CDCl_3$) δ: 163.3, 148.4, 145.6, 144.0, 136.3, 117.2, 113.7, 112.5, 102.6. High-resolution mass spectra (ESI) calcd for $C_9H_5Br_2O_3$ 320.8580 $[M + H]^+$, found 320.8582.

3,4-Dibromo-5-(2-thienylmethylene)-furan-2(5*H*)-one (3e, dr = 92:8)

Yield 40.5%. ^{1}H NMR (500 MHz, $CDCl_3$) δ: 7.61 (dd, J_1 = 5.0 Hz, J_2 = 0.5 Hz, 1H), 7.49 (dd, J_1 = 3.0 Hz, J_2 = 1.0 Hz, 1H), 7.12 (dd, J_1 = 5.0 Hz, J_2 = 1.0 Hz, 1H), 6.71 (s, 1H); ^{13}C NMR (125 MHz, $CDCl_3$) δ:162.8, 143.9, 136.0, 135.1, 133.2, 132.1, 130.2, 112.3, 107.7. High-resolution mass spectra (ESI) calcd for $C_9H_3Br_2O_2S$ 334.82054 $(M-H)^-$, found 334.82128.

General procedure for the synthesis of compounds 3f, 3g, 3h

To a solution of **2f** (0.174 g, 0.5 mmol) in anhydrous CH_3OH (7 mL) was added con. H_2SO_4 (0.01 g, 0.1 mmol). The mixture was stirred at 76 °C for 8 h under nitrogen, and then the mixture was concentrated in vacuo. The residue was washed by saturated Na_2CO_3 solution, exacted with CH_2Cl_2 (20 mL × 3), washed with brine, dried over Na_2SO_4, and concentrated in vacuo. The residue was purified by column chromatography on silica gel using ethyl acetate/petroleum ether (1:12) as the eluent to give compound **3f** (0.19 g, yield 60%) as a white solid. Compounds **3g** (0.11 g, yield 60%, yellow solid) and **3h** (0.12 g, yield 61%, yellow solid) were prepared from **2g** and **2h** using a similar procedure of **3f**.

3,4-Dibromo-5-(phenylmethylene)-furan-2(5*H*)-one (3f, dr = 90:10)

Yield 60%. MS (ESI) $[M + H]^+$ *m/z* 331; ^{1}H NMR (400 MHz, $CDCl_3$) δ: 7.10–7.84 (m, 5H,), 7.04(s, 0.10H), 6.4(s, 0.90H,). ^{13}C NMR(100 MHz, $CDCl_3$) δ: 162.8, 145.2, 137.0, 131.4, 130.6, 129.8, 128.6, 113.7, 112.7. High-resolution mass spectra (ESI) calcd for $C_{11}H_5Br_2O_2$ 328.86417 $(M-H)^-$, found 328.86457.

3,4-Dibromo-5-((3-nitrophenyl)methylene)-furan-2(5*H*)-one (3g, dr = 57:43)

Yield 60%. MS (ESI) $[M-H]^+$ *m/z* 374; ^{1}H NMR (500 MHz, $CDCl_3$) δ: 8.54(t, J_1 = 20.0 Hz, J_2 = 15.0 Hz, 0.57H), 8.17–8.34 (m, 1.71), 7.72 (dd, J_1 = 60.0 Hz, J_2 = 15.0 Hz, 0.43H), 7.57–7.68 (m, 1.29H), 7.03(s, 0.43H), 6.50 (s, 0.57H). ^{13}C NMR (125 MHz, $CDCl_3$) δ: 162.0, 146.3, 136.2, 134.9, 131.5, 129.1, 128.3, 124.3, 123.2, 119.8, 113.9, 109.8. High-resolution mass spectra (ESI) calcd for $C_{11}H_4Br_2NO_4$ 373.84927 $(M-H)^-$, found 373.84989.

3,4-Dibromo-5-((4-nitrophenyl)methylene)-furan-2(5*H*)-one (3h, dr = 82:18)

Yield 61%. ^{1}H NMR (500 MHz, $CDCl_3$) δ: 8.26(m, 2H), 7.96(dd, J_1 = 7 Hz, J_2 = 0.5 Hz, 1H), 7.58(dd, J_1 = 7 Hz, J_2 = 0.5 Hz, 1H), 7.02(s, 1H); ^{13}C NMR (125 MHz, $CDCl_3$) δ: 161.9, 147.9, 147.1, 137.6, 131.4, 131.2, 124.1, 123.4, 120.9, 115.4, 110.8. High-resolution mass spectra (ESI) calcd for $C_{11}H_4Br_2NO_4$ 373.84927 $(M-H)^-$, found 373.84925.

Procedure for the synthesis of compound 3i

To a solution of 3, 4-dibromo-2(5*H*)-furanone (**1b**) (0.173 g, 0.5 mmol) in anhydrous CH_3OH (7 mL) was added piperidine (0.009 g, 0.1 mmol) and 4-hydroxybenzaldehyde (0.073 g, 0.6 mmol). The mixture was refluxed for 1.5 h under nitrogen, and then the mixture was concentrated in vacuo. The residue was exacted with CH_2Cl_2 (20 mL × 3), washed with brine, dried over Na_2SO_4, and concentrated in vacuo. The residue was purified by column chromatography on silica gel using ethyl acetate/petroleum ether (1:15) as the eluent to give compound **3i** (0.05 g, yield: 29%) as a yellow solid.

3,4-Dibromo-5-((4-hydrophenyl)methylene)-furan-2(5*H*)-one (3i)

Yield 29%. ^{1}H NMR(400 MHz, $CDCl_3$) δ: 7.69(d, J = 8.7 Hz, 1H), 6.84(d, J = 8.7 Hz, 1H), 3.30(s, 1H); ^{13}C NMR (125 MHz, $CDCl_3$) δ: 162.1, 159.2, 142.1, 140.9, 133.2, 132.5, 122.9, 116.2, 116.1, 112.9. High-resolution mass spectra (ESI) calcd for $C_{11}H_7Br_2O_3$ 346.8736 $(M + H)^+$, found 346.8748.

Biological evaluation

Bacterial strains

Pseudomonas aeruginosa strains ATCC 27853, ATCC 9027, and PAOA (clinical isolates) were used to study the effects of new compounds to biofilm assay. A bacterial suspension made from fresh culture and aliquots were stored at −20 °C in glycerol and used within 2 weeks. Before used, bacterial suspensions were spread onto Mueller-Hinton solid medium and incubated at 37 °C for 18 h.

MIC determination

To define the concentration of the biofilm inhibitory test under MIC and make sure the effects of new compounds were via QS inhibition not inhibiting the bacteria themselves. The MICs of all compounds were measured. It was performed on planktonic cultures using the twofold dilution method according to clinical and laboratory standards[a]. MICs were performed in 96-well sterile microplates (cosmo), and the results were recorded after 18 h of incubation at 37 °C.

In vitro determination of biofilm formation

All the synthetic compounds as mentioned earlier were assayed for their *in vitro* bacterial biofilm formation inhibitory activities against *P. aeruginosa* ATCC 27853, ATCC 9027, and PAOA. Crystal violet staining method was used. *Pseudomonas aeruginosa* was diluted with LB broth at OD_{600} = 0.05. A concentrated compound solution was transferred into each well, except those used as controls, to achieve a final test concentration of 64 μg/mL, and each well was filled to a final volume of 200 μL. After 20 h of incubation at 35 °C and being washed twice with phosphate-buffered saline (PBS) solution, the biofilm remained on the wells was fixed with 200 μL of 99% methanol for 15 min. The solution was discarded and the microplate was put in super-clean bench. When the wells were dried, each of them was added with 250 μL of 1% solution of crystal violet (CV). After 15 min staining at room temperature, the wells were washed twice carefully with distilled solution. Then, 250 μL of 95% ethanol was added to each well, as to dissolve the stain and biofilm. Fifteen minutes later, the absorbance of plates was determined at 570 nm in a spectrophotometer. The percentage of biofilm inhibition was calculated using the following formula: inhibition percentage = $[(OD_{\text{negative control}} - OD_x)/OD_{\text{negative control}}] \times 100$, where x refers to the tested halogenated compounds (23–28).

To find out the effect of concentration on the QS system, some of the synthesized compounds were chosen to determine the biofilm inhibition percentages at concentrations of MIC, 1/2MIC, 1/4MIC, 1/8MIC, and 1/16MIC using the same method described earlier.

Observation of *Pseudomonas aeruginosa* biofilm formation with scanning electron microscopy (SEM)

The *P. aeruginosa* inoculums were centrifuged (11 100g, 5 min) and washed twice with saline to acquire planktonic cultures. It was diluted with sterile saline at 0.5 MCF (Mcfarland standard), and then diluted 25-fold with sterile saline. One milliliter of the prepared cultures was added to each test tube, as well as 1 mL compound solution (dissolved by LB broth, 128 μg/mL). The final concentration of compounds was 64 μg/mL. After the polyvinyl chloride catheter (0.5 cm × 0.5 cm) was set on the bottom of each tube, cultures were incubated in shaking bath at 37 °C for 7 days. Following washing twice with PBS solution, the bacteria on the catheter was fixed by placing in 2.5% glutaraldehyde/cacodylate (v/v) buffer for 5 h. The samples were then dried with ethanol steps – 50% aqueous ethanol (v/v) for 10 min, 75% aqueous ethanol (v/v) for 10 min, 85% aqueous ethanol (v/v) for 10 min, 95% aqueous ethanol (v/v) for 10 min, 100% aqueous ethanol (v/v) for 10 min, and isoamyl acetate for 10 min. They were frozen in a freezer at −65 °C and dried at the critical point of vacuum pressure at

−53 °C, and then covered with gold. Biofilms on the catheter were then observed with a SEM (29,30).

Molecular docking

As a widely used technology, molecular docking has become more and more important in drug design field. It is one of the essential tools to explain correlations between ligand structures and biological activities. Many studies (31) have revealed that QS inhibitors were targeted to the signal receptor LasR by binding into the pocket of the protein. Therefore, a molecular docking experiment was carried out to explore the binding mode between compounds and receptor LasR. Furanones designed here may proceed via covalent linkage between the bromine elements and the LuxS proteins (14); therefore, they were not appropriate for a molecular docking study, and LasR receptor of *P. aeruginosa* was only involved in this docking study. As the crystal structure of LasR in *P. aeruginosa* QS system was known, a systemic docking study was performed on these synthesized compounds.

The Surflex-Dock using an empirical scoring function and a patented search engine to dock ligands into a protein's binding site was applied to study molecular docking[b].

Crystal structure of LasR/AHL complex (PDB entry code: 2UV0) was obtained from RCSB Protein Data Bank (32). Three-dimensional structures of all compounds were constructed using the sketch molecular module. Structural energy minimization was performed using the standard Tripos molecular mechanics force field and Gasteiger-Hückel charge, and the max iteration for the minimization was set to 2000. The minimization was terminated when the energy gradient convergence criterion of 0.05 kcal/mol was reached. The moleculars used in the docking study were saved as SLN format. The automatic docking was applied to establish protomol, which meant that Surflex-Dock would find the largest cavity in the receptor protein. After AHLs and waters were removed, all the designed compounds were docked into the LasR-binding site by the empirical scoring function and the patented search engine in surflex-Dock. To visualize the binding mode between the protein and the ligand, the Molecular Computer Aided Design (MOLCAD) program was employed. MOLCAD calculated and displayed the surfaces of channels and cavities, as well as the separating surface between protein subunits. MOLCAD provided several surfaces to analyze correlations between compounds and receptor. The cavity depth (CD), the lipophilic potential (LP), and the electrostatic potential (EP) surfaces were generated, as well as robbin surfaces that illustrated the secondary structure elements of the binding structure of protein. Other parameters were as the default setting in the software.

Results and Discussion

Biological activity

The results of MIC were shown in Table 3. The compounds **1a** and **1b** showed an intermediate MIC (256 μg/mL) against ATCC 27853 and high MIC against strain PAOA. Compounds **2a**–**2c**, **2e**–**2h**, **3g**–**3i** bearing an aryl group at C-5 position showed decreased MIC values (512 μg/mL), whereas compounds **2d** and **2e** conjugated with nitrofuran moiety displayed a lower MIC of 128 μg/mL. Generally, the introduction of aryl groups has no significant influence on the MIC values of compounds against *P. aeruginosa*.

Table 3: MICs of synthesized compounds against *Pseudomonas aeruginosa* ATCC 27853, ATCC 9027, and PAOA[a]

	MIC (μg/mL)		
Compound	ATCC 27853	ATCC 9027	PAOA[a]
1a	256	128	512
1b	256	512	512
2a	512	512	512
2b	512	256	512
2c	256	256	512
2d	512	512	512
2e	128	128	512
2f	256	512	512
2g	256	512	512
2h	512	512	512
2i	64	256	256
3a	256	512	512
3e	512	512	512
3f	512	512	512
3g	512	>512	512
3h	512	512	512
3i	512	512	512
c	256	256	512
d	256	256	>512

[a]Clinical isolate.

Biofilm inhibition percentages of the synthesized compounds at the concentration of 64 μg/mL were illustrated in Table 4. Compounds **c** and **d** exhibited strong inhibitory effects on strain of ATCC 27853, and they also displayed weak inhibitory activities against ATCC 9027 and PAOA. Similar phenomenon was found in the cases of other compounds. It can be inferred that bacteria evolved and formed varies acceptors. Therefore, a strain was sensitive to certain compounds. Compared with compounds **c** and **d**, the synthesized compounds **2a**–**i** as well as **3a**–**i** were found to be less potential against strain ATCC 27853. However, some of them (e.g. **2f, 3f, 3i**) performed better inhibitory potencies on strain ATCC 9027 and PAOA. Meanwhile, some compounds (e.g., **2a**, **2b**, **3e**, **3h**) were negative toward one or two strains of *P. aeruginosa*, especially on PAOA.

The relationship between the concentrations and the effects of biofilm inhibition on *P. aeruginosa* ATCC 27853 was demonstrated in Figure 3. Inhibitory effects of **2h**, **3a**, **3f** descended as the concentration decreased (Figure 3), but the situation was opposite in the case of **2i**. A similar relationship between concentrations and effects was observed from some compounds, such as **2h**, **3a**, **3f**. Blackwell and co-workers (33,34) had revealed that compounds affecting QS system may act as antagonist or agonist when concentration changed significantly. As compounds acted to be an inhibitor or an activator was depended on the conformation of LasR-compound complex. Only when the conformation of LasR-compound was different from LasR-AHL, the compound may show inhibitory effect; otherwise, it may be an activator. Besides, one compound

Table 4: Biofilm inhibition of compounds at 64 μg/mL on *Pseudomonas aeruginosa*

Compound	Biofilm inhibition(%) at 64 μg/mL		
	ATCC 27853	ATCC 9027	PAOA
1a	–	14.2 ± 0.9△	46.7 ± 0.4**
1b	39.9 ± 1.9*	52.6 ± 1.8**	–
2a	30.1 ± 2.1*	8.90 ± 1.0△	–
2b	14.9 ± 2.5*	8.30 ± 1.0△	–
2c	5.93 ± 2.6*	–	18.1 ± 0.3*
2d	14.5 ± 2.4*	37.1 ± 0.9**	14.6 ± 0.6*
2e	9.15 ± 2.6*	15.8 ± 0.5**	–
2f	30.1 ± 2.1*	45.6 ± 2.0**	40.7 ± 0.7**
2g	35.2 ± 2.6*	39.0 ± 1.6**	–
2h	19.2 ± 1.5*	36.8 ± 1.1**	3.56 ± 0.6*
2i	–	58.7 ± 2.1**	34.1 ± 1.3**
3a	17.6 ± 2.0*	14.8 ± 1.1△	22.2 ± 0.7△
3e	–	30.0 ± 1.2**	–
3f	37.1 ± 1.9*	68.7 ± 0.9**	34.3 ± 1.4**
3g	23.5 ± 2.4*	27.7 ± 1.5**	–
3h	–	15.6 ± 1.2**	–
3i	41.3 ± 1.3*	71.8 ± 1.8**	38.9 ± 1.8**
c	57.4 ± 1.6△	–	23.6 ± 0.3△
d	51.6 ± 1.7	9.00 ± 1.6	25.8 ± 0.2

– Represents no inhibitory effect was observed. The absorbance was higher than the control group. *$p < 0.05$ versus controlled compound **d**, and biofilm inhibitions were smaller than controlled compound **d**. **$p < 0.05$ versus controlled compound **d**, and biofilm inhibitions were larger than controlled compound **d**. △$p > 0.05$ versus controlled compound **d**.

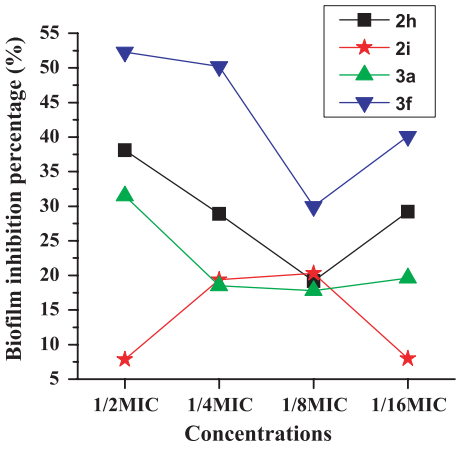

Figure 3: Different concentrations of biofilm inhibition on *Pseudomonas aeruginosa* ATCC 27853.

bonded and changed the conformation significantly, resulting in inhibitory effect at low concentrations. On the other hand, others possessing poor affinity with the receptor or forming a similar complex conformation showed certain inhibitory effect at high concentrations, or even some of them were partial agonist. It can be summarized that effects of compounds on QS system correlated with their concentrations closely.

The biofilm formation in the absence (control) or presence (**2i**, **3f**, **3i**) of halogenated furanone compounds were illustrated in Figure 4. Compared with the control, incubation of *P. aeruginosa* PAOA with compounds **2i, 3f, 3i** at a sub-MIC of 64 μg/mL resulted in obvious reduction of the biofilm.

Three strains of *P. aeruginosa* were applied to screen the inhibitory effects of compounds. It was found that the inhibitory effects of these compounds toward non-resistant strain and resistant strain were varied. Antibiotic-resistant phenotype variant underwent changes of gene expression; therefore, complicated mechanism may proceed in different strains. Further study would be needed to make a clear explanation. Recently, many new targets were found in QS system. Except the key receptor LasR in QS, RhlR, LuxS, and QscR (quorum-sensing-control repressor) have also been proved to be important. Multitarget compounds were designed here to discover potent inhibitors. As reported in literature (31), autoinducer-1 (AI-1) was QS signals of bacterium, AHLs for gram-negative bacteria, and oligopeptide for Gram-positive bacteria. Moreover, their QS mechanisms were strikingly disparate, whereas autoinducer-2 (AI-2) is signal of both Gram-negative and Gram-positive bacteria. Therefore, we assumed that AI-2 possessed a particular path to conduct QS, instead of binding LasR receptor. If one path was blocked and other ones were still open, the system may still work. Compounds inactivated LuxS would interfere the AI-2 path and block the producing of AI-2. More multi-target compounds should be designed to obstruct the whole QS system, in this way the potent inhibitors may be discovered.

Molecular docking analysis

All the tested molecular structures docked well to the binding site, and the structures that obtain high scores (**3f** = 7.31, **3i** = 6.95, **2f** = 6.85) were selected as the best molecules. In Figure 5, carbonyl of furanone formed hydrogen bonds with the $-NH_2$ of the Arg61, and hydroxyl in benzene ring formed hydrogen bond with Leu110. Hydrogen bonds may greatly increase the binding force between compounds and the receptor. Meanwhile, Figure 5 depicted the MOLCAD cavity depth potential surface of the binding site of LasR within compound (*Z*)-**3i**. The whole molecule in the light red color indicated that compound (*Z*)-**3i** were located deeply inside the LasR pocket. Figures 6 and 7 depicted the MOLCAD lipophilic potential and electrostatic potential surface binding site of LasR within compound (*Z*)-**3i**. As shown in Figure 6, the aromatic nucleus was found in a brown area, indicating that the lipophilic of the ring may increase the affinity of this molecular binding with LasR receptor. In Figure 7, the red color showed the electron-withdrawing zone and purple color showed electron-donating zone, and the carbonyl of furanone was in red area, playing the role of electron withdrawing. The aromatic ring of the compound (*Z*)-**3i** conjugated with furanone ring appearing to be electron donating, and also it was in the blue area, which was suitable to increase the activity of biofilm inhibition.

All designed compounds can dock well into the pocket of LasR receptor. Compounds that show potent activities in the bioassay obtain high scores in the molecular docking experiments. The high potency of (*Z*)-**3i** would attribute to the stabilization by the hydrogen bonds between the compound and residue Arg61, Leu110 of

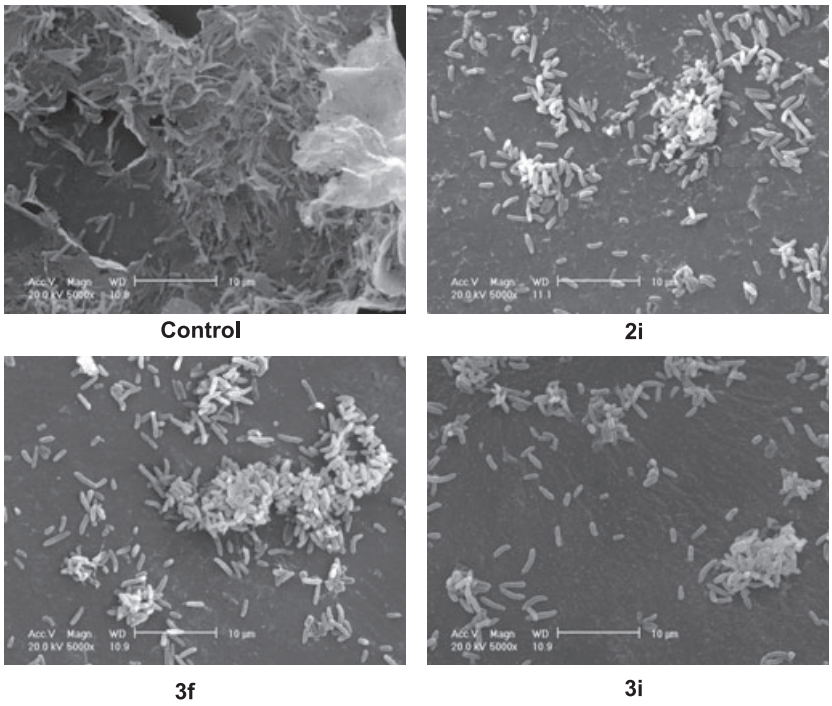

Figure 4: Scanning electron micrographs (5000×) of PAOA on the surface of catheter for 7 days in the absence (control) or presence of 64 μg/mL of compound **2i, 3f, 3i**..

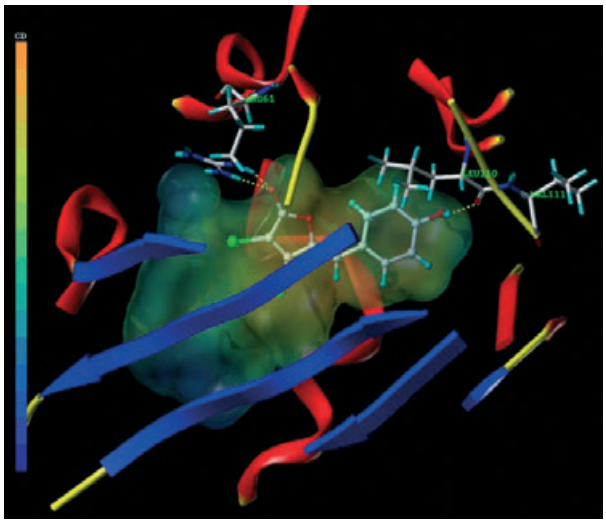

Figure 5: The Molecular Computer Aided Design robbin and multichannel potential surfaces structure displayed with cavity depth of the LasR pocket with compound (*Z*)-**3i**. Key residues and hydrogen bonds were labeled. The cavity depth color ramp ranges from blue (low depth values = outside of the pocket) to light red (high depth values = cavities deep inside the pocket).

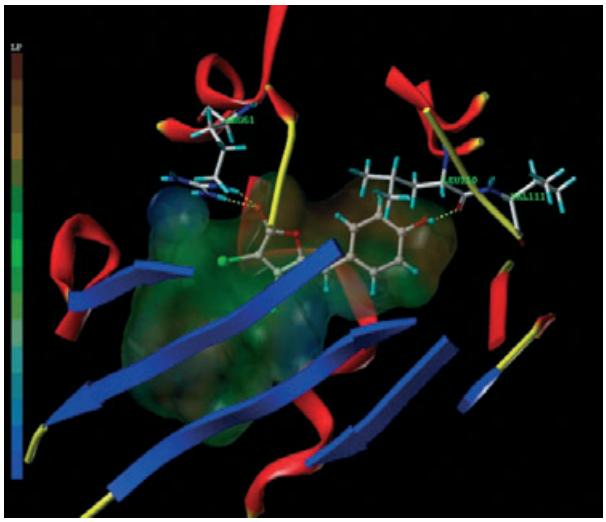

Figure 6: The Molecular Computer Aided Design lipophilic potential surfaces of LasR-binding site within compound (*Z*)-**3i**. key residues and hydrogen bonds were labeled. The brown represents highest lipophilic area, while blue indicated highest hydrophilic area.

LasR protein, together as well as by the lipophilic electron-donating aromatic ring.

This molecular docking made a try to identify some key structural features that were responsible for binding to LasR. The hydrogen bonds formed between structure and receptor protein may promote the binding affinity significantly. Therefore, it was helpful to introduce a substituted aromatic group as a side chain of halogenated furanones, especially the hydroxy-substituted ones.

Conclusions

In this study, a set of halogenated furanone compounds were designed and synthesized as biofilm inhibitors against *P. aerugin-*

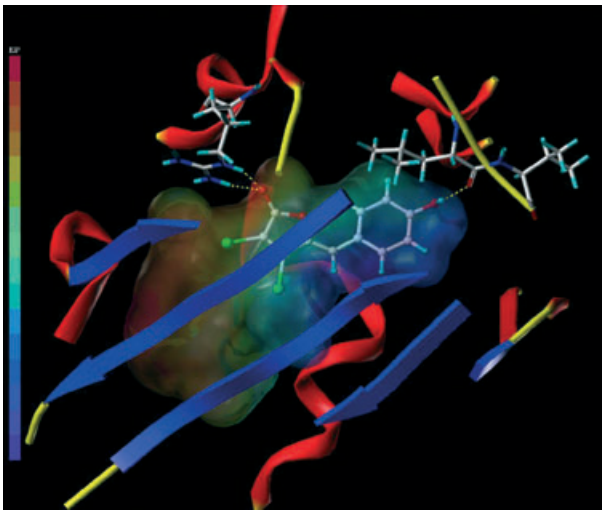

Figure 7: The Molecular Computer Aided Design electrostatic potential surfaces of LasR-binding site within compound (*Z*)-**3i**. Key residues and hydrogen bonds were labeled. The red color shows the electron-withdrawing zone and purple color shows electron-donating zone.

osa. The compounds **2i**, **3f**, **3i** showed remarkable effects of biofilm formation inhibition on *P. aeruginosa*. Molecular docking studies were employed to understand the binding site of the receptor LasR. The highest potency of (*Z*)-**3i** would be ascribable to the stabilization by the hydrogen bonds and lipophilic electron-donating aromatic ring.

Acknowledgments

This work was supported by the fund of Guangzhou technological project (NO. 2009J1-C271) and the National Natural Science Foundation of China (81072554). We gratefully acknowledge Dr. Weifeng Ma, Southern Medical University of China for kindly providing the *Pseudomonas aeruginosa* resistant strain (PAOA).

References

1. Fuqua W.C., Winans S.C., Greenberg E.P. (1994) Quorum sensing in bacteria – the LuxR-LuxI family of cell density-responsive transcriptional regulators. J Bacteriol;176:269–275.
2. Bjarnsholt T., Kirketerp-Moller K., Jensen P.O., Madsen K.G., Phipps R., Krogfelt K., Hoiby N., Givskov M. (2008) Why chronic wounds will not heal: a novel hypothesis. Wound Repair Regen;16:2–10.
3. Fu X.B. (2008) Bacterial biofilms and their roles in chronic skin ulcer development. J Trauma Surg;10:416–417.
4. James G.A., Swogger E., Wolcott R., Pulcini E.D., Secor P., Sestrich J., Costerton J.W., Stewart P.S. (2008) Biofilms in chronic wounds. Wound Repair Regen;16:37–44.
5. Davis S.C., Ricotti C., Cazzaniga A., Welsh E., Eaglstein W.H., Mertz P.M. (2008) Microscopic and physiologic evidence for biofilm-associated wound colonization in vivo. Wound Repair Regen;16:23–29.
6. Stewart P.S., Costerton J.W. (2001) Antibiotic resistance of bacteria in biofilms. Lancet;358:135–138.
7. Walters M.C., Roe F., Bugnicourt A., Franklin M.J., Stewart P.S. (2003) Contributions of antibiotic penetration, oxygen limitation, and low metabolic activity to tolerance of *Pseudomonas aeruginosa* biofilms to eiprofloxacin and tobramycin. Antimicrob Agents Chemother;47:317–323.
8. Fogerty M.D., Abumrad N., Nanney L., Arbogast P.G., Poulose B., Barbul A. (2008) Risk factors for pressure ulcers in acute care hospitals. Wound Repair Regen;16:11–18.
9. Musk D.J., Hergenrother P.J. (2006) Chemical countermeasures for the control of bacterial biofilms: effective compounds and promising targets. Curr Med Chem;13:2163–2177.
10. de Nys R., Steinberg P.D., Willemsen P., Dworjanyn S.A., Gabelish C.L., King R.J. (1995) Broad spectrum effects of secondary metabolites from the red alga *Delisea pulchra* in antifouling assays. Biofouling;8:259–271.
11. de Nys R., Wright A.D., Kongig G.M., Sticher O. (1993) New halogenated furanones from the marine alga *Delisea pulchra* (cf fimbriata). Tetrahedron;49:11213–11220.
12. Menefield M., de Nys R., Kumar N., Read R., Givskov M., Steinberg P., Kjelleberg S. (1999) Evidence that halogenated furanones from *Delisea pulchra* inhibit acylated homoserine lactone (AHL)-mediated gene expression by displacing the AHL signal from its receptor protein. Microbiology;145:283–291.
13. Ni N., Li M., Wang J., Wang B. (2009) Inhibitors and antagonists of bacterial quorum sensing. Med Res Rev;29:65–124.
14. Zang T.Z., Lee B.W.K., Cannon L.M., Ritter K.A., Dai S., Ren D., Wood T.K., Zhou Z.S. (2009) A naturally occurring brominated furanone covalently modifies and inactivates LuxS. Bioorg Med Chem Lett;19:6200–6204.
15. Geske G.D., Mattmann M.E., Blackwell H.E. (2008) Evaluation of a focused library of *N*-aryl L-homoserine lactones reveals a new set of potent quorum sensing modulators. Bioorg Med Chem Lett;18:5978–5981.
16. Ube H., Shimada N., Terada M. (2010) Asymmetric direct vinylogous aldol reaction of furanone derivatives catalyzed by an axially chiral guanidine base. Angew Chem Int Ed Engl;49:1858–1861.
17. Sarma K.D., Zhang J., Curran T.T. (2006) Novel synthons from mucochloric acid: the first use of α,β-dichloro-γ-butenolides and γ-butyrolactams for direct vinylogous aldol addition. J Org Chem;72:3311–3318.
18. Bang S.C., Kim Y., Yun M.Y., Ahn B.Z. (2004) 5-Arylidene-2(*5H*)-furanone derivatives: synthesis and structure-activity relationship for cytotoxicity. Arch Pharm Res;27:485–494.
19. Ravi P.S., Bruce M.F., Li D. (2010) Asymmetric vinylogous aldol reaction of silyloxy furans with a chiral organic salt. J Am Chem Soc;132:9558–9560.
20. Hjelmgaard T., Persson T., Rasmussen T.B., Givskov M., Nielsen J. (2003) Synthesis of furanone-based natural product analogues with quorum sensing antagonist activity. Bioorg Med Chem;11:3261–3271.
21. Bellina F., Rossi R. (2007) An efficient and inexpensive multigram synthesis of 3,4-dibromo- and 3,4-dichlorofuran-2(5*H*)-one. Synthesis;12:1887–1889.

22. Li X., Huang M., Chen Q. (2000) Synthesis and structure of the novel chiral 4-dialkyloxyphosphpnyl-2(5*H*)-furanones. Acta Chimi Sin;3:363–367.
23. Ramsey M.M., Whiteley M. (2004) *Pseudomonas aeruginosa* attachment and biofilm development in dynamic environments. Mol Microbiol;53:1075–1087.
24. Knezevic P., Petrovic O. (2008) A colorimetric microtiter plate method for assessment of phage effect on *Pseudomonas aeruginosa* biofilm. J Microbiol Meth;74:114–118.
25. Stepanovic S., Vukovic D., Dakic I., Savic B., Svabic-Vlahovic M. (2000) A modified microtiter-plate test for quantification of staphylococcal biofilm formation. J Microbiol Meth;40:175–179.
26. Ying Y.C., Lee K.C. (2005) The burkholderia pseudomallei BpeAB-OprB efflux pump: expression and impact on quorum sensing and virulence. J Bacteriol;14:4707–4719.
27. Abdi-Ali A., Mohammadi-Mehr M., Agha Alaei Y. (2006) Bactericidal activity of various antibiotics against biofilm-producing *Pseudomonas aeruginosa*. Int J Antimicrob Agents;27:196–200.
28. Fonseca A.P., Sousa J.C. (2007) Effect of shear stress on growth, adhesion and biofilm formation of *Pseudomonas aeruginosa* with antibiotic-induced morphological changes. Int J Antimicrob Agents;30:236–241.
29. Baveja J.K., Willcox M.D.P., Hume E.B.H., Kumar N., Odell R., Poole-Warren L.A. (2004) Furanones as potential anti-bacterial coatings on biomaterials. Biomaterials;25:5003–5012.
30. Tré-Hardy M., Vanderbist F., Traore H., Devleeschouwer M.J. (2008) In vitro activity of antibiotic combinations against *Pseudomonas aeruginosa* biofilm and planktonic cultures. Int J Antimicrob Agents;31:329–336.
31. Rasmussen T.B., Givskov M. (2006) Quorum-sensing inhibitors as anti-pathogenic drugs. Int J Med Microbiol;296:149–161.
32. Bottomley M.J., Muraglia E., Bazzo R., Carfi A. (2007) Molecular insights into quorum sensing in the human pathogen *Pseudomonas aeruginosa* from the structure of the virulence regulator LasR bound to its autoinducer. J Biol Chem;282:13592–13600.
33. Geske G.D., O'Neill J.C., Miller D.M., Wezeman R.J., Mattmann M.E., Lin Q., Blackwell H.E. (2008) Comparative analyses of N-acylated homoserine lactones reveal unique structural features that dictate their ability to activate or inhibit quorum sensing. Chembiochem;9:389–400.
34. Mattmann M.E., Geske G.D., Worzalla G.A., Chandler J.R., Sappington K.J., Greenberg E.P., Blackwell H.E. (2008) Synthetic ligands that activate and inhibit a quorum-sensing regulator in *Pseudomonas aeruginosa*. Bioorg Med Chem Lett;18:3072–3075.

Notes

[a]National Committee for Clinical Laboratory Standards (2009) Performance standards for antimicrobial susceptibility testing; nineteenth in formational supplement. M100-S19.
[b]SYBYL 8.1. Tripos Inc., St. Louis, USA.